Stabilization variation of organic conductor surfaces induced by π–π stacking interactions*

Dou Rui-Fen(窦瑞芬)[a], Lin Feng(林 峰)[b], Liu Fu-Wei(刘富伟)[a], Sun Yi(孙 祎)[a], Yang Ji-Yong(杨继勇)[a], Lin Bing-Fa(林炳发)[a], He Lin(何 林)[a], Xiong Chang-Min(熊昌民)[a], and Nie Jia-Cai(聂家财)[a]†

[a] *Department of Physics, Beijing Normal University, Beijing* 100875, *China*

[b] *School of Physics, State Key Laboratory for Mesoscopic Physics, Peking University, Beijing* 100871, *China*

(Received 27 December 2011; revised manuscript received 13 January 2012)

The structures and stabilization of three crystal surfaces of TCNQ-based charge transfer complexes (CTCs) including $PrQ(TCNQ)_2$, $MPM(TCNQ)_2$, and $MEM(TCNQ)_2$, have been investigated by scanning tunneling microscopy (STM). The three bulk-truncated surfaces are all *ac*-surface, which are terminated with TCNQ molecular arrays. On the *ac*-surface of $PrQ(TCNQ)_2$, the TCNQ molecules form a tetramer structure with a wavelike row behavior and a γ angle of about 18° between adjacent molecules. Moreover, the dimer structures are resolved on both *ac*-surfaces of $MPM(TCNQ)_2$ and $MEM(TCNQ)_2$. In addition, the tetramer structure is the most stable structure, while the dimer structures are unstable and easily subject to the STM tip disturbance, which results in changeable unit cells. The main reasons for the surface stabilization variation among the three *ac*-surfaces are provided by using the 'π-atom model'.

Keywords: charge transfer complex (CTC), scanning tunneling microscopy (STM), π–π stacking interaction, stabilization

PACS: 68.37.Ef, 82.45.Jn, 82.75.Fq **DOI:** 10.1088/1674-1056/21/5/056801

1. Introduction

Organic charge-transfer complexes (CTCs) and their derivatives, have been intensively investigated because of appealing physical properties in electronics,[1−3] optics,[4,5] and magnetics.[6,7] In particular, the CTCs, such as (7,7,8,8-tetracyanoquino dimethane)-based species, have been confirmed to have potential applications in optical and electronic memory devices[8−11] as well as switches.[12,13] For the TCNQ-based complexes, it is well known that the complexes have a layer structure consisting of a π-donor layer alternating with an acceptor one, in which the packing structures of the donor or acceptor are controlled by the π–π stacking interactions.[14] The studies on the relationship between CTC crystal structures and their physical properties have revealed that the novel properties predominantly depend on their packing patterns formed by donor or acceptor molecular layers.[13,15] Recently, most studies are related to the bulk prosperities of TCNQ-based CTCs and surface reconstruction.[16−22] However, the question of how π–π stacking interactions determine the molecular packing characteristics on the acceptor or donor molecular layer and the resulting surface stability is seldom investigated. Moreover, due to the symmetry broken on the crystal surfaces, molecular packing structures of CTCs can be different from those in the bulk, which finally provides a new insight into the mechanism of charge transfer and the origin of physical properties.[13]

In the present paper, we shall study three bulk-truncated surfaces of TCNQ-based CTCs, that is, N-propylpyridinium-quino bis-7,7,8,8-tetracyanoquino dimethane ($PrQ(TCNQ)_2$), N-methyl-N-propylmorpholinium bis-7,7,8,8-tetracyanoquino dimethane ($MPM(TCNQ)_2$), and N-methyl-N-ethylmorpholinium bis-7,7,8,8-tetracyanoquino dimethane ($MEM(TCNQ)_2$), by using scanning tunneling microscopy (STM). We find that all bulk-truncated surfaces of three complexes are *ac*-surfaces terminated with arrays of TCNQ molecular chains along

*Project supported by the National Natural Science Foundation of China (Grant Nos. 10804010, 50772015, 60977015, and 10974019), the National Basic Research Program of China (Grant No. 2006CB932301), and the Scientific Research Foundation for the Returned Overseas Chinese Scholars of Ministry of Education.

†Corresponding author. E-mail: jcnie@bnu.edu.cn

© 2012 Chinese Physical Society and IOP Publishing Ltd

the c axis. However, because of different donor bases which induce changeable interactions between the acceptor and donor in these three molecular crystals, the TCNQ molecular packing characteristics can be different among the three CTC *ac*-surfaces. For TCNQ π-molecule, the intermolecular interactions are mainly dominated by the parallel-displaced π–π stacking interactions, which have been known to be the dominant force in stabilizing the double helical structures of DNA, the tertiary structures of proteins, and the large ordered π-system molecular self-assembly monolayers.[23−27] Therefore, to reveal the molecular packing states of individual TCNQ molecules on different acceptor molecular layers and to explore the stability of three kinds of molecular layer is very important for constructing the relationship between the structural stability and the interaction between TCNQ molecules, which may lead to a deeper understanding of the organic conductors and their applications in molecular electronics.

2. Experimental section

A serial of organic conductors based on the TCNQ component of $PrQ(TCNQ)_2$, $MPM(TCNQ)_2$, and $MEM(TCNQ)_2$ were synthesized with the method of Melby.[28] As reported earlier,[21] the clean bulk-truncated surfaces of $PrQ(TCNQ)_2$, $MPM(TCNQ)_2$, and $MEM(TCNQ)_2$ were freshly *as*-grown crystal surfaces. After the CTC crystals were fixed in the alloy plates by the silver glue, these plates were loaded into an ultrahigh vacuum chamber with a base pressure of about 5×10^{-10} mbar for STM (UNISOKU) measurements. All STM images were taken at room temperature in a constant-current scanning mode with a tunneling current of 0.2–0.5 nA and a bias voltage of 40–80 mV (with respect to the samples). The STM tips were mechanically cut from a wire of Pt(80%)Ir(20%) alloys. Lateral dimensions observed in the STM images were calibrated with a highly-ordered pyrolytic graphite (HOPG) standard.

3. Results and discussion

3.1. Comparison of the surface structures of three CTCs

3.1.1. Surface structure of the $PrQ(TCNQ)_2$ crystal

The crystal structure of $PrQ(TCNQ)_2$ determined by the X-ray diffraction at room temperature is triclinic with the unit-cell parameters: $a = 7.53(2)$ Å, $b = 15.15(2)$ Å, $c = 14.30(4)$ Å; $\alpha' = 1111.2(1)°$, $\beta' = 88.9(5)°$, and $\gamma' = 99.1(6)°$, in which the TCNQ chains lie along the c axis.[29] The left part in Fig. 1(a) shows that the bulk-truncated *ac*-surface is terminated with arrays of TCNQ chains along the c axis. Individual TCNQ molecules are in the stand-upright form along the long molecular axis of TCNQ, with two nitrogen atoms on the outermost surface. There are four TCNQ molecules along the c axis in a unit cell, exhibiting a tetramer structure with step-by-step increase of height for each molecule. As reported earlier,[19,30] there are two distinct face-to-face stacking modes between neighboring molecules in the TCNQ chains. The external-to-ring (two molecules slipped by about 2.1 Å along the long axis) and shifted external-to-ring motifs are shown at the top-right corner and bottom-right corner in Fig. 1(a), respectively.

To clarify the molecular packing details of the crystal surface, we study the clean $PrQ(TCNQ)_2$ single crystal by using STM. Figure 1(b) shows a large-size STM image of the $PrQ(TCNQ)_2$ surface. It is found that this surface exhibits a molecular flat terrace with few defects. The cursor line A crossing the step, as shown in Fig. 1(c), displays the step height of about 14.825 Å, which agrees with the unit length of the b axis well (15.15 Å). Hence, this surface should correspond to the *ac*-surface ({010}). The molecular flat terraces should be terminated with TCNQ molecules.

A zoom-in STM image is obtained on the flat terrace, as shown in Fig. 2(a). Obviously, an individual TCNQ molecule can be resolved as one bright dot and four bright protrusions form a unit cell. Based on the TCNQ packing features in the bulk structure, the bright dot must correspond to a nitrogen atom in the outermost surface because the long axis of TCNQ is not exactly perpendicular to the c axis. According to the STM image, the unit cell marked by green solid lines can be obtained: $a = 7.48$ Å, $c = 15.07$ Å, and $\beta' = 90.5°$, which are in good agreement with the crystal structure obtained by the X-ray diffraction, $a = 7.532$ Å, $c = 14.304$ Å, and $\beta' = 88.9(5)°$. Thus, the surface is a bulk-truncated *ac*-surface. The four bright protrusions observed form a TCNQ tetramer, which indeed reflects the structural features from the bulk. The average distance between two adjacent TCNQ molecules along the c axis is about 3.77 Å, which is very close to the *ab initio* calculation.[31,32]

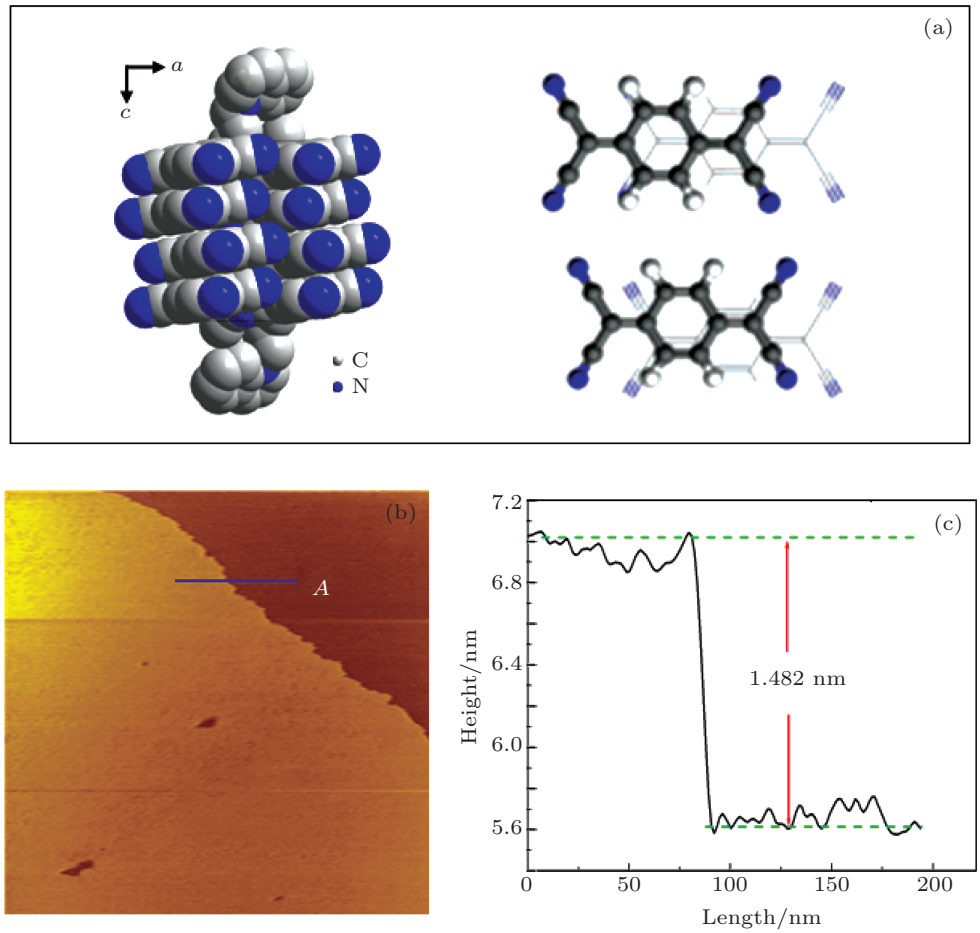


Fig. 1. (colour online) (a) Left: structure of the bulk-truncated *ac*-surface of $PrQ(TCNQ)_2$; Right: space-filling model of the bulk-truncated *ac*-surface of $PrQ(TCNQ)_2$ terminated with the TCNQ chains along the *c* axis. Two stacking modes in TCNQ chains are defined as "external-to-ring" and "shifted external-to-ring" motifs, respectively. (b) Large-scale STM image (130×130 nm^2) of the *ac*-surface of the $PrQ(TCNQ)_2$crystal with $V = -40$ mV and $I = 0.34$ nA. (c) The cursor line *A* in Fig. 1 (b) shows the height profile along the single terrace.

Interestingly, the resolved TCNQ molecules in the *ac*-surface for $PrQ(TCNQ)_2$ are not precisely parallel to each other, but take on wave-like rows with a slight tilted angle of about 18° between neighboring molecules (labeled by two crossed yellow lines along the short molecular axis). To date, this molecular packing characteristic has not been referred to in the TCNQ-based CTCs. Actually, it has been shown that large π-molecules (anthryl-based molecules) prefer to form the wavelike row structures in our previous papers.[25,26] The driving force for the formation of wavelike rows is that the intermolecular π–π interactions prefer a nonzero γ angle, which has been discussed in detail elsewhere.[25,26] At present, the appearance of a wavelike structure with a tilted angle in the TCNQ system provides, once more, an evidence to confirm the above-mentioned conclusion that the wavelike rows can form only if the tilted γ angle is nonzero in large π-systems.[25,26]

In the case of the $PrQ(TCNQ)_2$ crystal surface, the center-center separation R_{CEN},[24] the parallel-displacement angle θ,[24] and the tilted angle γ[24] between two neighboring TCNQ molecules along the *c* axis are about 3.77 Å, 30°, and 18°, respectively. Compared with the data obtained for protein,[24] DNA,[23] and the self-assembled anthracene-based monolayers,[25,26] these values exactly fall into the packing rule of two parallel π molecules with an offset distance and a tilted angle controlled predominantly by the parallel-displaced π–π interactions.

Since the electrons mainly distribute in the double bonds in the TCNQ, a TCNQ molecule can be schematically drawn, as shown in Fig. 2(b). This model in Fig. 2 visually interprets the formation mechanism of the TCNQ wavelike rows with a period of four molecules. In this case, the presence of a constant angle θ is due to the energy-favored offset π-stacking.[30] More importantly, the γ angle of 18° is the key point

for the formation of the wavelike TCNQ rows. In other words, in a large π-system including protein, DNA, and molecular crystals, a nonzero γ angle ($< 30°$) is a common molecular packing feature confined by the parallel-displaced π–π stacking interactions.

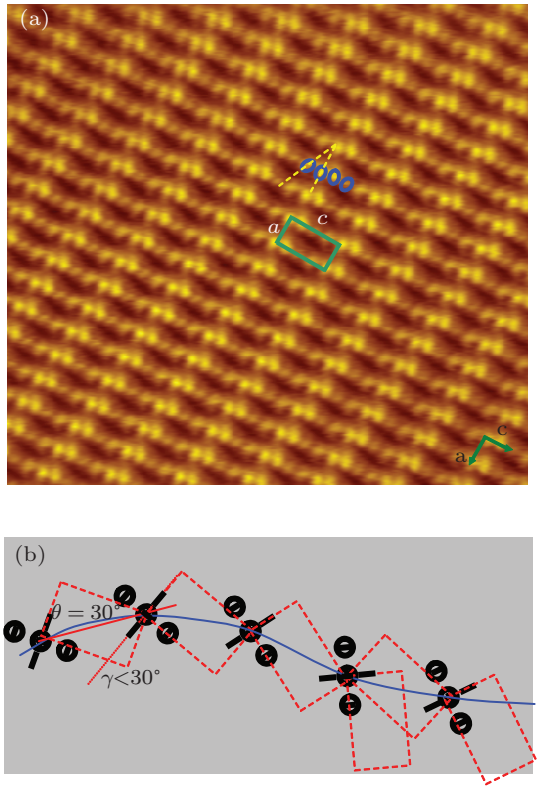


Fig. 2. (colour online) (a) High-resolution STM image (14×14 nm^2) of the *ac*-surface of PrQ(TCNQ)$_2$. ($V = -49$ mV, $I = 0.33$ nA). The blue ovals in the image represent the molecular orientation of a single TCNQ along the *c* axis. The yellow lines through the TCNQ short axis reveal that two neighbouring molecules along the *c* axis are packed with a nonzero γ angle. The green quadrilateral is a unit cell in the *ac*-surface. (b) Schematic molecular structure based on the molecular packing features shown by Fig. 2(a).

3.1.2. Surface structure of the MPM (TCNQ)$_2$ crystal

The crystal structure of MPM(TCNQ)$_2$ determined via the X-ray diffraction is triclinic, with the unit-cell parameters: $a = 7.862(1)$ Å, $b = 28.518(3)$ Å, $c = 6.560(1)$ Å; $\alpha' = 90.23(1)°$, $\beta' = 75.71(1)°$, and $\gamma' = 91.44(1)°$ at room temperature.[32] The bulk-truncated *ac*-surface is presented on the left in Fig. 3(a), which is terminated with arrays of TCNQ along the *c* axis. In one unit cell, two TCNQ molecules with a stand-upright configuration along the long molecular axis are not located in the same height along the *c* axis. Moreover, two TCNQ molecules along the *c* axis are slightly shifted to each other by a face-to-face distance of 3.28 Å (see the left part in Fig. 3(b)) to compromise for parallel-displaced π–π stacking interactions. These two shifted TCNQ molecules form a dimer structure. The nearest spacing along the *c* axis almost equals the optimal π–π stacking distance of 3.4–3.6 Å.[27] Due to the relative strong π–π overlapping, the *ac*-surface has the lowest surface free energy and is stable enough to be easily identified.

Figure 3(b) is a large-size STM image of the crystal surface of MPM(TCNQ)$_2$, which presents a molecular flat terrace. The cursor line "*A*" crossing a step is shown in Fig. 3(c). The step height is about 23.85 Å, which is roughly consistent with the unit length of the *b* axis, 28.518 Å. Hence, this surface corresponds to the {010} *ac*-surface. The molecular flat terraces should be terminated with TCNQ molecules.

Figures 4(a) and 4(b) show two zoomed-in STM images obtained on the same scanning region with the same scanning parameters of -46.6 mV and 0.29 nA. One TCNQ molecule is resolved as a bright dot because two nitrogen atoms in one TCNQ molecule are not in the same lateral level. Furthermore, the dimer structure can be resolved in Fig. 4(a). A slightly bright protrusion between two bright dots along the *c* axis can be resolved, which corresponds to the lower TCNQ molecule in the shifted dimer structure. The unit cell marked by a green quadrilateral "A" in Fig. 4(a) can be obtained: $a = 8.70$ Å, $c = 5.08$ Å, and $\beta' = 73.7°$. This unit cell lattice deviates a bit from that of the *ac*-surface structure obtained via the X-ray diffraction: $a = 7.862$ Å, $c = 6.560$ Å, and $\beta' = 75.71°$.

After scanning the same area for a long interval, we obtain an STM image, as shown in Fig. 4(b). The unit cell obtained from Fig. 4(b) is completely different from that in Fig. 4(a). It tells that the crystal lattice marked by the quadrilateral "A'" is $a = 8.72$ Å, $c = 7.28$ Å, and $\beta' = 86.8°$. This means that the *ac*-surface in the MPM(TCNQ)$_2$ crystal is unstable and readily induced by external stimuli, such as the scanning force or the electrical field. Even though the fact that the surface structural variation can be induced by the STM tip has been reported, the fundamental reasons are not provided in the Ref. [17]. The reasons for the structural variation in the *ac*-surface for the MPM(TCNQ)$_2$ crystal will be discussed below in detail.

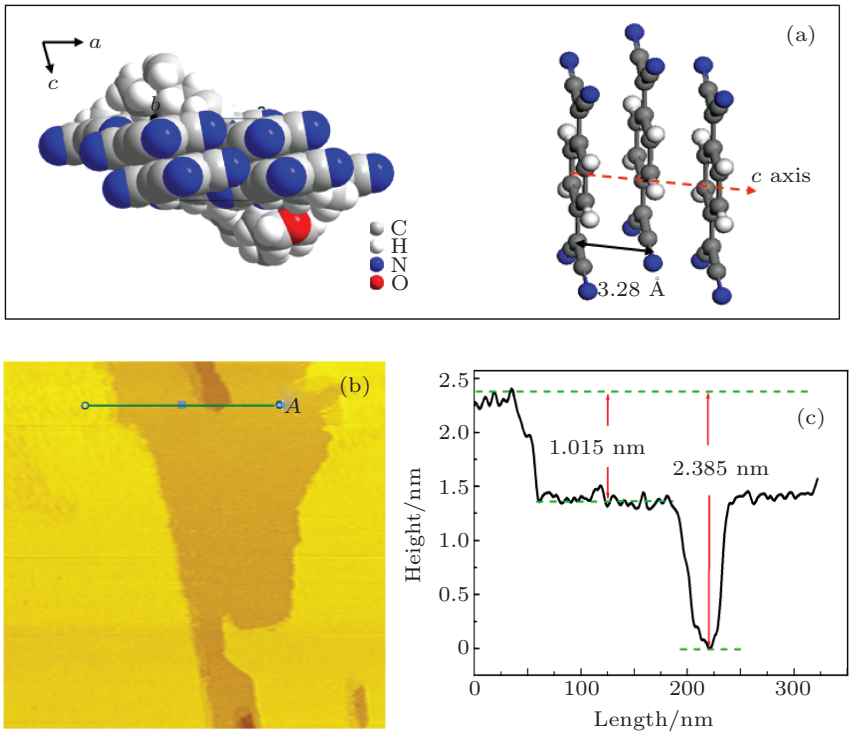


Fig. 3. (colour online) (a) Structure of the bulk-truncated *ac*-surface of MPM(TCNQ)$_2$. Left: space-filling model of the bulk-truncated *ac*-surface of MPM(TCNQ)$_2$ terminated with the TCNQ chains along the *c* axis. Right: stacking mode for the formation of a dimer by two TCNQ molecules. (b) Large-scale STM image of the *ac*-surface of PrQ(TCNQ)$_2$ ($V = -51$ mV, $I = 0.27$ nA). (c) The cursor line *A* in the Fig. 3 (b) shows the height profile along the single terrace.

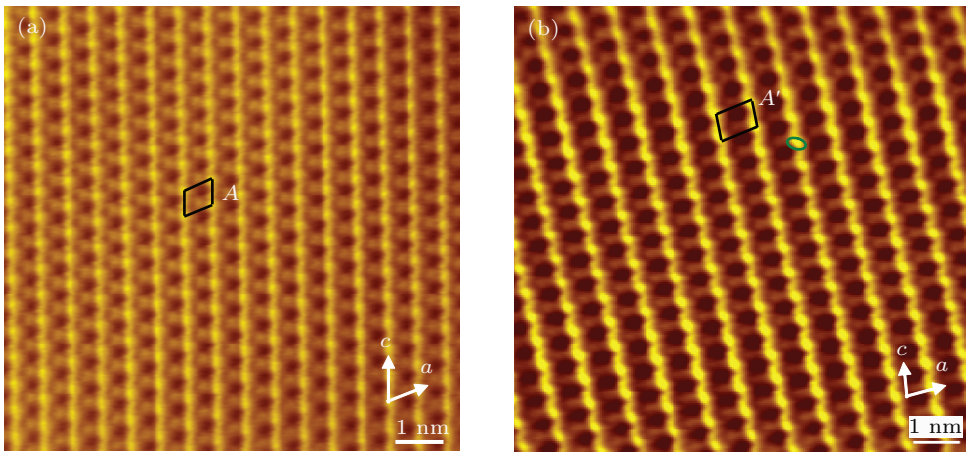


Fig. 4. (colour online) (a) High-resolution STM image of *ac*-surface of MPM(TCNQ)$_2$. (b) High-resolution STM image after a long interval obtained in the same area as Fig. 4(a). ($V = -46$ mV, $I = 0.29$ nA). The STM image sizes (12×12 nm^2) of Figs. 4(a) and 4(b) are the same. Two green quadrilaterals represent different unit cells in the *ac*-surface, respectively. A green oval in Fig. 4(b) labels one TCNQ molecule.

3.1.3. Surface structure of the MEM(TCNQ)$_2$ crystal

The crystal structure of MEM(TCNQ)$_2$ determined by the X-ray diffraction is triclinic and very analogous to that of MPM(TCNQ)$_2$ with the parameters $a = 7.824(5)$ Å, $b = 15.426(16)$ Å, $c = 6.896(5)$ Å, and $\alpha' = 113.59(8)°$, $\beta' = 73.27(7)°$, $\gamma' = 112.71(8)°$ at room temperature.[17,34] The *ac*-surface of MEM(TCNQ)$_2$ is very similar to that of MPM(TCNQ)$_2$, thus the schematic structure of the bulk-truncated *ac*-surface can be shown in Fig. 3(a). Two TCNQ molecules along the *c* axis are slightly

shifted to each other with a neighboring distance of 3.45 Å, which also corresponds to the optimal π–π stacking distance of 3.4–3.6 Å.[27]

Figure 5 is a large-size STM image of the surface of the MEM(TCNQ)$_2$ crystal, which also displays a molecular flat terrace. However, the size of the terrace is not particularly large. The height profile of "A" in the inset of Fig. 5(a) tells the step height of about 15.45 Å, which is consistent with the unit length of the b axis (15.42 Å). Thus, we can conclude that this surface is the {010} ac-surface of the MEM(TCNQ)$_2$ crystal. Analogous to the ac surface for MPM(TCNQ)$_2$, the structural variation also occurs in the MEM(TCNQ)$_2$ ac-surface with the increase of scanning interval.

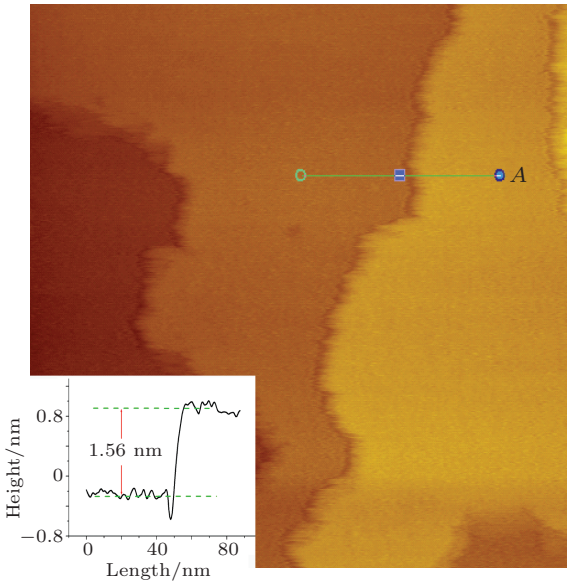


Fig. 5. (colour online) Large-scale STM image (100 × 100 nm^2) of the ac-surface for MEM(TCNQ)$_2$ ($V = -35.8$ mV, $I = 0.37$ nA). This STM image shows that the step edge is not very clear. The inset shows the height profile along the single terrace step.

Figures 6(a) and 6(b) show the STM images obtained on the same scanning region with a scanning bias voltage of −36 mV and a tunneling current of 0.38 nA. From Fig. 6(a), the crystal lattice "A" is obtained: $a = 7.90$ Å, $c = 6.42$ Å, and $\beta' = 80.2°$, which is very close to the ac-surface structure obtained via the X-ray diffraction, $a = 7.824$ Å, $c = 6.896$ Å, and $\beta' = 73.27°$. However, from Fig. 6(b), another crystal lattice "A'" is obtained: $a = 8.46$ Å, $c = 6.83$ Å, and $\beta' = 66.5°$. The reasons for the existence of two surface structures are discussed below.

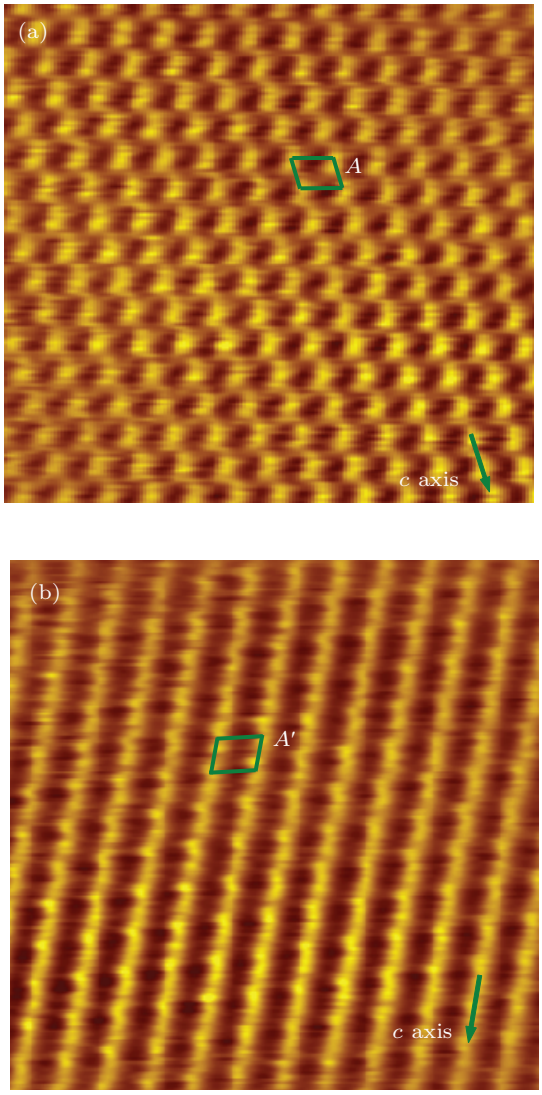


Fig. 6. (colour online) High-resolution STM images of ac-surface for MEM(TCNQ)$_2$ at the same scanning conditions ($V = -36$ mV, $I = 0.38$ nA). The scanning area for Figs. 6(a) and 6(b) is 12 × 12 nm^2 and 10 × 10 nm^2, respectively. Two green quadrilaterals represent two different unit cells in the ac-surface.

3.2. Comparison of surface stabilities for three CTCs

To examine the stability of the wavelike row structure with a tetramer periodicity in the PrQ(TCNQ)$_2$ ac-surface, we change the scanning parameters, i.e., increase the tunneling currents, to make the STM tip approach the surface as close as possible. In contrast to the ac-surface of MPM(TCNQ)$_2$ and MEM(TCNQ)$_2$ (see Figs. 4 and 6), the ac-surface of PrQ(TCNQ)$_2$ is quite stable without being altered at different scanning parameters. This implies that the surface structure formed by four TCNQ molecules in the ac-surface of PrQ(TCNQ)$_2$ is much more stable

compared with the dimer TCNQ structures in the *ac*-surface of both MPM(TCNQ)$_2$ and MEM(TCNQ)$_2$ crystals.

Here, we propose that the stabilization of the tetramer structure originates from the wave-like row structure with a constant θ and a nonzero tilted γ angle. This packing structure should be the energy-favored packing mode. As we have discussed above, the formation of the TCNQ wavelike row in the *ac*-surface for the PrQ(TCNQ)$_2$ crystal is controlled by the strong parallel-displaced π–π interactions. To understand this packing model, once again, we rely on the idea of 'π-atom model',[27] in which the σ framework and π electrons are considered separately. The favorable interaction is actually the π–σ attraction that overcomes the π–π repulsion and prefers an offset or slipped geometry. On the basis of this idea and Fig. 2(b), a non-zero angle indeed introduces a relative shift and reduces the π-electron overlap a bit, which means that π–π repulsion can be suppressed to a certain degree. Consequently, the intermolecular π–π interactions are enhanced compared with those in the dimer structure without the nonzero γ angle. Therefore, the tetramer structure is quite stable and can endure the external stimuli such as the thermal perturbation, the mechanical force generated by the tip, and even the external electrical field. In the same way, in the TEA(TCNQ) crystal, it is not found that the tetramer structure can be changed during the scanning measurement.[21] On the contrary, the stabilization of *ac*-surfaces of MPM(TCNQ)$_2$ and MEM(TCQN)$_2$ crystals is relatively weak and easily influenced by the external stimuli. Another point worthy of noting is that the strong π–π interactions between TCNQ molecules play a key role in enhancing the electron transfer in the acceptor-layer surface. This fact has been proved by the electrical conductivity in the PrQ(TCNQ)$_2$ *ac*-surface being better than that in the MPM(TCNQ)$_2$ and MEM(TCNQ)$_2$ *ac*-surfaces.[20,22]

4. Conclusion

In summary, we have investigated three *ac*-surfaces of TCNQ-based CTCs by using STM. The high-resolution STM results reveal that TCNQ molecules form a tetramer structure with a wavelike shape and a tilted γ angle between adjacent molecules in the *ac*-surface for the PrQ(TCNQ)$_2$ crystal. However, the TCNQ molecules are packed into a dimer structure in the *ac*-surface of MPM(TCNQ)$_2$ and MEM(TCNQ)$_2$ crystals. The TCNQ tetramerization is the most stable structure and the molecular packing state is independent of the scanning parameters. However, the dimerized TCNQ structure on both MPM(TCNQ)$_2$ and MEM(TCNQ)$_2$ *ac*-surfaces is unstable. Through analyzing the TCNQ packing characteristics on the tetramer and dimer structures, we provide a rational elucidation to the structural stability of different CTC *ac*-surfaces. For the wavelike tetramer structure, the enhanced intermolecular π–π interactions originating from the TCNQ molecular parallel-displaced arrangement with a nonzero angle between two neighboring molecules, facilitate the formation of stable surface structures.

References

[1] Koch N, Duhm S, Rabe J P, Vollmer A and Johnson R L 2005 *Phys. Rev. Lett.* **95** 237601

[2] Jaeckel F, Watson M D, Muellen K and Rabe J P 2004 *Phys. Rev. Lett.* **92** 188303

[3] Muller R, Naulaerts R, Billen J, Genoe J and Heremans P 2007 *Appl. Phys. Lett.* **90** 063503

[4] Rath A K, Dhara K, Banerjee P and Pal A J 2008 *Langmuir* **24** 5937

[5] Chollet M, Guerin L, Uchida N, Fukaya S, Shimoda H, Ishikawa T, Matsuda K, Hasegawa T, Ota A, Yamochi H, Saito G, Tazaki R, Adachi S and Koshihara S 2005 *Science* **30** 86

[6] Narymbetov B, Omerzu A, Kabanov V V, Tokumoto M, Kobayashi H and Mihailovic D 2000 *Nature* **407** 883

[7] Blundell S J and Pratt F L 2004 *J. Phys. Condens. Matter* **16** R771

[8] Liu Y, Ji Z Y, Tang Q X, Jiang L, Li H X, He M, Hu W P, Zhang D Q, Wang X K, Wang C, Liu Y Q and Zhu D B 2005 *Adv. Mater.* **17** 2953

[9] Ouyang C, Guo Y B, Liu H B, Zhao Y J, Li G X, Li Y J, Song Y L and Li Y L 2009 *J. Phys. Chem.* C **113** 7044

[10] Reda T, Collings A F, Barton C and Lukins P 2003 *J. Phys. Chem.* B **107** 13774

[11] Zhou X, Pfeiffer M, Blochwitz J, Werner A, Nollau A, Fritz T and Leo K 2001 *Appl. Phys. Lett.* **78** 410

[12] O'Mullane A P, Fay N, Nafady A and Bond A M 2007 *J. Am. Chem. Soc.* **129** 2066

[13] Jaeckel F, Perera U G E, Iancu V, Braun K F, Koch N, Rabe J P and Hla S W 2008 *Phys. Rev. Lett.* **100** 126102

[14] Shibaeva R P and Yagubskii E B 2004 *Chem. Rev.* **104** 5347

[15] Horiuchi S, Okimoto Y, Kumai R and Tokura Y 2003 *Science* **299** 229

[16] Cui S, Li Y, Guo Y, Liu H, Song Y, Xu J, Lü J, Zhu M and Zhu D B 2008 *Adv. Mater.* **20** 309

[17] Dvorak M A, Li S L and Ward M D 1994 *Chem. Mater.* **6** 1386

[18] Quivy A, Deltour R, Bentum P J M, Gerritsen J W, Jansen A G M and Wyder P 1995 *Surf. Sci.* **325** 185

[19] Li S L, White H S and Ward M D 1992 *Chem. Mater.* **4** 1082
[20] Huang X M, Lin F, Zhou W, Ren L, Peng H and Liu Z F 2008 *J. Phys. Chem.* C **112** 2004
[21] Lin F, Zhou W, Huang X M, Ren L and Liu Z F 2008 *J. Phys. Chem.* C **112** 1090
[22] Peng H L and Liu Z F 2010 *Coord. Chem. Rev.* **254** 1151
[23] Saenger W 1984 *Principles of Nucleic Acid Structure* (New York: Pringer-Verlag) p. 261
[24] McGarughey G B, Gagne M and Rappe A K 1998 *J. Bio. Chem.* **273** 15458
[25] Dou R F, Ma X C, Xi L, Yip X L, Wong K Y, Lau W M, Jia J F, Xue Q K, Yang W S, Ma H and Jen A K Y 2006 *Langmuir* **22** 3049
[26] Dou R F, Ma X C, Xi L, Yip X L, Wong K Y, Lau W M, Fan X L, Jia J F, Xue Q K, Yang W S, Ma H and Jen A K Y 2008 *J. Phys: Condens. Matter* **20** 315017
[27] Hunter C A and Sanders J K M 1990 *J. Am. Chem. Soc.* **112** 5525
[28] Melby L R, Harder R J, Hertler W R, Mahler W, Benson R E and Mochel W E 1962 *J. Am. Chem. Soc.* **84** 3374
[29] Herbstein F H 2005 *Crystalline Molecular Complexes and Compounds: Structures and Principles* (Oxford: Oxford University Press)
[30] Filhol A and Thomas M 1984 *Acta Cryst. Sect.* B **40** 44
[31] Lee N K, Park S and Kim S K 2000 *J. Chem. Phys.* **116** 7902
[32] Lee N K, Park S and Kim S K 2000 *J. Chem. Phys.* **116** 7910
[33] Visser B R J J, De B J L and Vos A 1990 *Acta Cryst. Sect.* C **46** 857
[34] Bosch A and Van Bodegom B 1977 *Acta Cryst. Sect.* B **33** 3013